

Compact finite difference schemes for the backward fractional Feynman-Kac equation with fractional substantial derivative

Jiahui Hu(胡嘉卉)[1,2], Jungang Wang(王俊刚)[1], Yufeng Nie(聂玉峰)[1], Yanwei Luo(罗艳伟)[2]
Citation: Chin. Phys. B . 2019, 28(10): 100201 . **doi:** 10.1088/1674-1056/ab3af3
Journal homepage: http://cpb.iphy.ac.cn; http://iopscience.iop.org/cpb

What follows is a list of articles you may be interested in

Heteroclinic cycles in a new class of four-dimensional discontinuous piecewise affine systems

Wenjing Xu(徐文静), Wei Xu(徐伟), Li Cai(蔡力)
Chin. Phys. B . 2018, 27(11): 110201 . **doi:** 10.1088/1674-1056/27/11/110201

Finite-difference time-domain modeling of curved material interfaces by using boundary condition equations method

Jia Lu(卢佳), Huaichun Zhou(周怀春)
Chin. Phys. B . 2016, 25(9): 090203 . **doi:** 10.1088/1674-1056/25/9/090203

A meshless scheme for partial differential equations based on multiquadric trigonometric B-spline quasi-interpolation

Gao Wen-Wu, Wang Zhi-Gang
Chin. Phys. B . 2014, 23(11): 110207 . **doi:** 10.1088/1674-1056/23/11/110207

An interpolating reproducing kernel particle method for two-dimensional scatter points

Qin Yi-Xiao, Liu Ying-Ying, Li Zhong-Hua, Yang Ming
Chin. Phys. B . 2014, 23(7): 070207 . **doi:** 10.1088/1674-1056/23/7/070207

An improved local radial point interpolation method for transient heat conduction analysis

Wang Feng, Lin Gao, Zheng Bao-Jing, Hu Zhi-Qiang
Chin. Phys. B . 2013, 22(6): 060206 . **doi:** 10.1088/1674-1056/22/6/060206

Compact finite difference schemes for the backward fractional Feynman–Kac equation with fractional substantial derivative*

Jiahui Hu(胡嘉卉)[1,2], Jungang Wang(王俊刚)[1], Yufeng Nie(聂玉峰)[1,†], and Yanwei Luo(罗艳伟)[2]

[1] Department of Applied Mathematics, Northwestern Polytechnical University, Xi'an 710129, China
[2] College of Science, Henan University of Technology, Zhengzhou 450001, China

(Received 15 June 2019; revised manuscript received 23 July 2019; published online 30 September 2019)

The fractional Feynman–Kac equations describe the distributions of functionals of non-Brownian motion, or anomalous diffusion, including two types called the forward and backward fractional Feynman–Kac equations, where the nonlocal time–space coupled fractional substantial derivative is involved. This paper focuses on the more widely used backward version. Based on the newly proposed approximation operators for fractional substantial derivative, we establish compact finite difference schemes for the backward fractional Feynman–Kac equation. The proposed difference schemes have the q-th $(q = 1,2,3,4)$ order accuracy in temporal direction and fourth order accuracy in spatial direction, respectively. The numerical stability and convergence in the maximum norm are proved for the first order time discretization scheme by the discrete energy method, where an inner product in complex space is introduced. Finally, extensive numerical experiments are carried out to verify the availability and superiority of the algorithms. Also, simulations of the backward fractional Feynman–Kac equation with Dirac delta function as the initial condition are performed to further confirm the effectiveness of the proposed methods.

Keywords: backward fractional Feynman–Kac equation, fractional substantial derivative, compact finite difference scheme, numerical inversion of Laplace transforms

PACS: 02.60.–x, 02.60.Cb, 02.70.Bf **DOI:** 10.1088/1674-1056/ab3af3

1. Introduction

Diffusive motions exist widely in the nature, among the fields from condensed matter physics,[1–3] to hydrodynamics,[4] meteorology,[5] and finance.[6] Thus the Brownian functionals play important role in science community. Assume that $x(t)$ is a path of a Brownian particle in the time interval $(0,t)$, and $U(x)$ is some prescribed function. Then a Brownian functional can be defined as $A = \int_0^t U(x(\tau))\,\mathrm{d}\tau$. Since $x(t)$ is a random path, A is a random variable. On account of the diversity of the function $U(x)$, the Brownian functional A models various phenomena. In 1949, by using Feynman's path integral method, Kac derived the (imaginary time) Schrödinger equation for the distribution function of A.[7] However, in recent years, by realizing that numerous anomalous diffusion phenomena exist widely in many systems,[8,9] the scientists pay more and more attention to the anomalous diffusion processes, or the non-Brownian motion, which can be modeled more exactly by fractional differential equations.[10]

Let $x(t)$ be a trajectory of non-Brownian particle. The functional of anomalous diffusion has the same form as the Brownian functional

$$A = \int_0^t U(x(\tau))\,\mathrm{d}\tau. \tag{1}$$

For the different prescribed function $U(x)$, various physics processes can be characterized. For instance, when taking $U(x) = 1$ in a given domain and to be zero otherwise, A models the time spent by a particle in the domain. The corresponding functional can be used in kinetic studies of chemical reactions that take place exclusively in the domain.[11,12] When the motion of the particles is non-Brownian in dispersive systems with inhomogeneous disorder, $U(x)$ is given by x or x^2.[12] By employing a versatile framework for describing the motion of particles in disordered systems, *i.e.*, the continuous time random walk (CTRW), derived the forward and backward fractional Feynman–Kac equations,[12–14] where the fractional substantial derivative is involved. The fractional substantial derivative is a time–space coupled operator, which is different from other fractional derivatives such as the Caputo and Riemann-Liouville types, and this newly proposed definition will be described in Definition 2. Both the forward and backward fractional Feynman–Kac equations describe the distributions of functionals of the widely observed subdiffusive processes. While in most cases scholars are only interested in the distribution of the functional A and regardless of the final position of the particle, it turns out to be more convenient to use the backward version. The backward fractional Feynman–Kac equation which is shown in Eq. (2), will be discussed detailedly in our work. Denote by $P(x,A,t)$ the joint probability density function (PDF) of A and x at time t, which implies the

*Project supported by the National Natural Science Foundation of China (Grant No. 11471262) and Henan University of Technology High-level Talents Fund, China (Grant No. 2018BS039).

†Corresponding author. E-mail: yfnie@nwpu.edu.cn

© 2019 Chinese Physical Society and IOP Publishing Ltd

process has started at x and the particle is found on A at time t. The backward fractional Feynman–Kac equation is given as[12–14]

$$\frac{\partial}{\partial t}P(x,\rho,t) = K_\alpha {}^sD_t^{1-\alpha}\frac{\partial^2}{\partial x^2}P(x,\rho,t) - \rho U(x)P(x,\rho,t), \quad (2)$$

where $P(x,\rho,t) := \int_0^\infty P(x,A,t)\,\mathrm{e}^{-\rho A}\,\mathrm{d}A$, $\Re(\rho) > 0$, $U(x) \geq 0$; the functional A is defined as Eq. (1) and $\alpha \in (0,1)$; the diffusion coefficient K_α is a positive constant, and the symbol ${}^sD_t^\nu$ represents the fractional substantial derivative of order ν.[15]

For the past few years, numerical methods for solving fractional partial differential equations (PDEs) have been well developed, including finite difference methods,[16–20] finite element methods,[21–23] mixed finite element methods,[24,25] finite volume methods,[26,27] mixed finite volume element method,[28] and spectral methods,[29,30] *etc*. However, as for the PDEs with fractional substantial derivative involved, though there have been some literature for getting the numerical solutions (see Ref. [31]), high order finite difference schemes with the maximum norm error estimates have not been investigated yet. As is well known, high order schemes lead to more accurate results and less cost in computations if the solution of the equation is regular enough. Also, compared with the error estimates in discrete L^2 norm, the discrete L^∞ norm error estimates provide more immediate insight on the error occurring during time evolution. Thus, in practice, error estimates in the grid-independent maximum norm are preferred in numerical analysis. Noticing that the fractional substantial derivative is a non-local time–space coupled operator, it may bring more difficulty in constructing high order schemes for solving the corresponding equations, as well as in establishing the maximum norm error analysis. The purpose of this work is to develop efficient finite difference schemes for the backward fractional Feynman–Kac equation, which can achieve the q-th $(q = 1,2,3,4)$ order accuracy in temporal direction and the fourth order accuracy in spatial direction, respectively. The numerical stability and convergence in the maximum norm are discussed afterwards. Abundant numerical examples are also carried out to show the feasibility and the superiority of the proposed schemes.

The definitions of fractional substantial calculus are given as follows.[32]

Definition 1 Let $\nu > 0$, ρ be a constant, and $P(t)$ be piecewise continuous on $(0,\infty)$ and integrable on any finite subinterval of $[0,\infty)$. Then the fractional substantial integral of $P(t)$ of order ν is defined as

$${}^sI_t^\nu P(t) = \frac{1}{\Gamma(\nu)}\int_0^t (t-\tau)^{\nu-1}\,\mathrm{e}^{-\rho U(x)(t-\tau)}P(\tau)\,\mathrm{d}\tau, \quad t > 0, \quad (3)$$

where $U(x)$ is a prescribed function in Eq. (1).

Definition 2 Let $\mu > 0$, ρ be a constant, and $P(t)$ be $(m-1)$-times continuously differentiable on $(0,\infty)$ and its m-times derivative be integrable on any finite subinterval of $[0,\infty)$, where m is the smallest integer that exceeds μ. Then the fractional substantial derivative of $P(t)$ of order μ is defined as

$${}^sD_t^\mu P(t) = {}^sD_t^m[{}^sI_t^{m-\mu}P(t)], \quad (4)$$

where

$${}^sD_t^m = \left(\frac{\partial}{\partial t} + \rho U(x)\right)^m. \quad (5)$$

According to the definition of fractional substantial derivative, equation (2) can be expressed in the following form

$${}^sD_t^1 P(x,\rho,t) = {}^sD_t^{1-\alpha}\left[K_\alpha\frac{\partial^2}{\partial x^2}P(x,\rho,t)\right]. \quad (6)$$

Denote by ${}_c^sD_t^\alpha$ the Caputo fractional substantial derivative,[32] *i.e.*,

$$\begin{aligned}{}_c^sD_t^\alpha P(x,t) :&= {}^sD_t^\alpha\left[P(x,t) - \mathrm{e}^{-\rho U(x)t}P(x,0)\right]\\ &= {}^sD_t^\alpha P(x,t) - \frac{t^{-\alpha}\,\mathrm{e}^{-\rho U(x)t}}{\Gamma(1-\alpha)}P(x,0),\end{aligned}$$

and then the equivalent form of Eq. (6) can be written as[31]

$${}_c^sD_t^\alpha P(x,t) = K_\alpha\frac{\partial^2}{\partial x^2}P(x,t), \quad (7)$$

where $P(x,\rho,t)$ is replaced by $P(x,t)$ since ρ is given as a fixed constant. In the following two sections, we still use $P(x,t)$ for convenience.

The remainder of this paper is organized as follows. In Section 2, for the backward fractional Feynman–Kac equation, the compact finite difference schemes with temporal q-th $(q = 1,2,3,4)$ order accuracy and spatial fourth order accuracy are established. In Section 3, by generalizing the inner product in Ref. [18] to complex space, we prove the unconditional stability and convergence of the first-order time discretization scheme in the maximum norm. In Section 4, extensive numerical examples are provided to verify the effectiveness and accuracy of the proposed schemes from the first to the fourth order time discretization. In particular, simulations of the backward fractional Feynman–Kac equation with Dirac delta function as the initial condition are carried out to further confirm the feasibility of the proposed methods. Finally we draw some conclusions in the last section.

2. Derivation of compact difference schemes

This section focuses on deriving compact difference schemes for the backward fractional Feynman–Kac equation, which are of the q-th $(q = 1,2,3,4)$ order approximation in temporal direction and the fourth order approximation in spatial direction, respectively.

Without loss of generality, consider the backward fractional Feynman–Kac equation with a non-homogeneous source term in the interval $\Omega = (0, L)$,

$$\begin{aligned} {}_c^s D_t^\alpha P(x,t) :&= {}^s D_t^\alpha \left[P(x,t) - \mathrm{e}^{-\rho U(x) t} P(x,0) \right] \\ &= K_\alpha \frac{\partial^2}{\partial x^2} P(x,t) + f(x,t), \\ &\quad 0 < t \le T,\ x \in \Omega, \end{aligned} \tag{8}$$

and the initial and boundary conditions are given as

$$P(x,0) = \varphi(x), \quad x \in \Omega, \tag{9}$$

$$P(0,t) = \psi_1(t), \quad P(L,t) = \psi_2(t), \quad 0 \le t \le T. \tag{10}$$

Let M and N be two positive integers, then $h = L/M$ and $\tau = T/N$ are the uniform size of spatial grid and time step, respectively. A spatial and temporal partition can be defined as $x_i = ih$ for $i = 0, 1, \ldots, M$, and $t_n = n\tau$ for $n = 0, 1, \ldots, N$. Denote $\Omega_h = \{x_i \mid 0 \le i \le M\}$ and $\Omega_\tau = \{t_n \mid 0 \le n \le N\}$. Take $\mathcal{V}_h = \{u | u = (u_0, u_1, \ldots, u_M), u_0 = u_M = 0\}$ as the grid function space on Ω_h. Then for any grid function $u \in \mathcal{V}_h$, we have the following notations

$$\delta_x u_{i-1/2} = \frac{1}{h}(u_i - u_{i-1}), \quad \delta_x^2 u_i = \frac{1}{h}(\delta_x u_{i+1/2} - \delta_x u_{i-1/2}),$$

$$\mathcal{H}_h u_i = \begin{cases} \frac{1}{12}(u_{i+1} + 10u_i + u_{i-1}), & 1 \le i \le M-1, \\ u_i, & i = 0 \ \text{ or } \ M. \end{cases}$$

It can be observed that $\mathcal{H}_h u_i = (1 + \frac{h^2}{12}\delta_x^2) u_i$ for $1 \le i \le M-1$. For any $u, v \in \mathcal{V}_h$, taking $\bar{v}$ as the complex conjugate of v, we introduce an inner product by generalizing the inner product in Ref. [18] to complex space

$$\begin{aligned} \langle u, v \rangle &= h \sum_{i=0}^{M-1} (\delta_x u_{i+1/2})(\delta_x \bar{v}_{i+1/2}) \\ &\quad - \frac{h^2}{12} h \sum_{i=1}^{M-1} (\delta_x^2 u_i)(\delta_x^2 \bar{v}_i), \end{aligned} \tag{11}$$

which can be verified directly according to the definition of inner product. Also, some norms which are necessary for the numerical analysis are shown below

$$\|u\|_\infty = \max_{1 \le i \le M-1} |u_i|, \quad \|u\| = \sqrt{h \sum_{i=1}^{M-1} |u_i|^2},$$

$$\|\delta_x^2 u\| = \sqrt{h \sum_{i=1}^{M-1} |\delta_x^2 u_i|^2}, \quad \|\delta_x u\| = \sqrt{h \sum_{i=1}^{M} |\delta_x u_{i-1/2}|^2}. \tag{12}$$

For the inner product (11) and above norms, we have the following lemmas.

Lemma 1 For $\forall u \in \mathcal{V}_h$, we have

$$\frac{2}{3}\|\delta_x u\|^2 \le \langle u, u \rangle \le \|\delta_x u\|^2.$$

Proof From Eqs. (11) and (12), we obtain

$$\langle u, u \rangle = \|\delta_x u\|^2 - \frac{h^2}{12}\|\delta_x^2 u\|^2, \tag{13}$$

which shows $\langle u, u \rangle \le \|\delta_x u\|^2$ immediately.

On the other hand, we have

$$\begin{aligned} h^2 \|\delta_x^2 u\|^2 &= h \sum_{i=1}^{M-1} |\delta_x u_{i+1/2} - \delta_x u_{i-1/2}|^2 \\ &\le 2h \sum_{i=1}^{M-1} \left(|\delta_x u_{i+1/2}|^2 + |\delta_x u_{i-1/2}|^2 \right) \\ &\le 4\|\delta_x u\|^2. \end{aligned} \tag{14}$$

Combining Eq. (13) with inequality (14), it is derived

$$\langle u, u \rangle \ge \frac{2}{3}\|\delta_x u\|^2.$$

This completes the proof.

Lemma 2 (Inequality (8.4.1) in Ref. [33]) For $\forall u \in \mathcal{V}_h, \|u\|_\infty \le \sqrt{L}/2 \|\delta_x u\|$.

Lemma 3 (Lemma 4.1 in Ref. [34]) Let function $g(x) \in C^6[a,b]$ and $\xi(\lambda) = 5(1-\lambda)^3 - 3(1-\lambda)^5$. Then

$$\begin{aligned} \mathcal{H}_h g''(x_i) &= \delta_x^2 g(x_i) + \frac{h^4}{360} \int_0^1 [g^{(6)}(x_i - \lambda h) \\ &\quad + g^{(6)}(x_i + \lambda h)] \xi(\lambda) \mathrm{d}\lambda, \quad 1 \le i \le M-1. \end{aligned}$$

According to Ref. [32], the fractional substantial derivatives appeared in Eq. (8) have q-th order approximations, *i.e.*,

$${}^s D_t^\alpha P(x,t)|_{(x_i,t_n)} = \frac{1}{\tau^\alpha} \sum_{k=0}^{n} d_{i,k}^{q,\alpha} P(x_i, t_{n-k}) + \mathcal{O}(\tau^q), \tag{15}$$

$$\begin{aligned} &{}^s D_t^\alpha [\mathrm{e}^{-\rho U(x) t} P(x,0)]_{(x_i,t_n)} \\ &= \frac{1}{\tau^\alpha} \sum_{k=0}^{n} d_{i,k}^{q,\alpha} \mathrm{e}^{-\rho U_i (n-k)\tau} P(x_i, 0) + \mathcal{O}(\tau^q), \end{aligned} \tag{16}$$

where

$$U_i = U(x_i)$$

and

$$d_{i,k}^{q,\alpha} = \mathrm{e}^{-\rho U_i k \tau} l_k^{q,\alpha}, \quad q = 1, 2, 3, 4. \tag{17}$$

$l_k^{1,\alpha}$, $l_k^{2,\alpha}$, $l_k^{3,\alpha}$, and $l_k^{4,\alpha}$ are defined in Ref. [35]. For the sake of completeness, we list them below. First of all, $l_k^{1,\alpha}$ is given by a recursively formula

$$l_0^{1,\alpha} = 1, \quad l_k^{1,\alpha} = \left(1 - \frac{\alpha+1}{k}\right) l_{k-1}^{1,\alpha}, \quad k \ge 1. \tag{18}$$

Taking $\mathrm{i} = \sqrt{-1}$, there are

$$l_k^{2,\alpha} = \left(\frac{3}{2}\right)^\alpha \sum_{m=0}^{k} \left(\frac{1}{3}\right)^m l_m^{1,\alpha} l_{k-m}^{1,\alpha}, \quad k \ge 0,$$

and

$$l_k^{3,\alpha} = \left(\frac{11}{6}\right)^\alpha \sum_{j=0}^{k} \sum_{m=0}^{j} \mu_3^m \overline{\mu_3}^{j-m} l_m^{1,\alpha} l_{j-m}^{1,\alpha} l_{k-j}^{1,\alpha}, \quad k \ge 0,$$

where $\mu_3 = 4/(7 + \sqrt{39}\mathrm{i})$ and $\overline{\mu_3} = 4/(7 - \sqrt{39}\mathrm{i})$.

Denote

$$\nu_4 = \frac{3a}{-b-(\sqrt[3]{Y_1}-\sqrt[3]{-Y_2})};$$
$$\mu_4 = \frac{3a}{-b+(1/2)(\sqrt[3]{Y_1}-\sqrt[3]{-Y_2})+(\sqrt{3}/2)(\sqrt[3]{Y_1}+\sqrt[3]{-Y_2})\mathrm{i}};$$
$$\overline{\mu_4} = \frac{3a}{-b+(1/2)(\sqrt[3]{Y_1}-\sqrt[3]{-Y_2})-(\sqrt{3}/2)(\sqrt[3]{Y_1}+\sqrt[3]{-Y_2})\mathrm{i}},$$

where $a=-3/25$, $b=13/25$, $c=-23/25$, $d=1$; $A=b^2-3ac$, $B=bc-9ad$, $C=c^2-3bd$; $\Delta=B^2-4AC>0$, $Y_1=Ab+(3/2)a(-B-\sqrt{\Delta})>0$, $Y_2=Ab+(3/2)a(-B+\sqrt{\Delta})<0$, then

$$l_k^{4,\alpha} = \left(\frac{25}{12}\right)^{\alpha}\sum_{n=0}^{k}\sum_{j=0}^{n}\sum_{m=0}^{j}\nu_4^{k-n}\mu_4^{m}\overline{\mu_4}^{j-m}l_m^{1,\alpha}l_{j-m}^{1,\alpha}l_{n-j}^{1,\alpha}l_{k-n}^{1,\alpha},\quad k\geq 0.$$

Considering Eq. (8) at the point (x_i,t_n), it can be written as

$${}_c^sD_t^{\alpha}P(x_i,t_n) = K_{\alpha}\frac{\partial^2 P(x_i,t_n)}{\partial x^2}+f(x_i,t_n).$$

Acting the compact operator $\mathcal{H}_h$ on both sides of the above equation, we have

$$\mathcal{H}_h\left({}_c^sD_t^{\alpha}P(x_i,t_n)\right) = K_{\alpha}\mathcal{H}_h\frac{\partial^2 P(x_i,t_n)}{\partial x^2}+\mathcal{H}_h f(x_i,t_n). \quad (19)$$

Assuming $u(x,t)\in C_{6,2}^{x,t}([0,L]\times[0,T])$, by use of Eqs. (15), (16), and Lemma 3, we obtain

$$\begin{aligned}&\mathcal{H}_h\left(\frac{1}{\tau^{\alpha}}\sum_{k=0}^{n}d_{i,k}^{q,\alpha}P(x_i,t_{n-k})\right.\\&\left.-\frac{1}{\tau^{\alpha}}\sum_{k=0}^{n}d_{i,k}^{q,\alpha}\,\mathrm{e}^{-\rho U_i(n-k)\tau}P(x_i,0)\right)\\&= K_{\alpha}\delta_x^2P(x_i,t_n)+\mathcal{H}_h f(x_i,t_n)+R_i^n, \quad (20)\end{aligned}$$

where $R_i^n=\mathcal{H}_h(R_t^{\alpha})_i^n+K_{\alpha}(R_x)_i^n$ with $(R_t^{\alpha})_i^n=\mathcal{O}(\tau^q)$ and

$$(R_x)_i^n = \frac{h^4}{360}\int_0^1\left[\frac{\partial^6 P}{\partial x^6}(x_i-\lambda h,t_n)+\frac{\partial^6 P}{\partial x^6}(x_i+\lambda h,t_n)\right]\xi(\lambda)\,\mathrm{d}\lambda.$$

Therefore there exists a constant $\widetilde{C}$ such that

$$|R_i^n|\leq\widetilde{C}(\tau^q+h^4),\quad q=1,2,3,4. \quad (21)$$

Denote by P_i^n the approximated value of $P(x_i,t_n)$, and $f_i^n=f(x_i,t_n)$. Multiplying Eq. (20) by τ^{α}, and omitting the small term, we derive the compact difference schemes for solving the backward fractional Feynman–Kac equation (8) with the initial condition (9) and boundary condition (10) as follows:

$$\begin{aligned}&\mathcal{H}_h\sum_{k=0}^{n}d_{i,k}^{q,\alpha}P_i^{n-k}-\mathcal{H}_h\sum_{k=0}^{n}d_{i,k}^{q,\alpha}\,\mathrm{e}^{-\rho U_i(n-k)\tau}P_i^0\\&= K_{\alpha}\tau^{\alpha}\delta_x^2P_i^n+\tau^{\alpha}\mathcal{H}_h f_i^n,\\&\quad 1\leq i\leq M-1,\ \ 1\leq n\leq N,\ \ q=1,2,3,4, \quad (22)\\&\quad P_i^0=\varphi(x_i),\quad 1\leq i\leq M-1, \quad (23)\\&\quad P_0^n=\psi_1(t_n),\quad P_M^n=\psi_2(t_n),\quad 0\leq n\leq N. \quad (24)\end{aligned}$$

To execute the procedure, we rewrite Eq. (22) as the following equivalent form

$$\begin{aligned}&\mathcal{H}_h d_{i,0}^{q,\alpha}P_i^n-\frac{K_{\alpha}\tau^{\alpha}}{h^2}\left(P_{i+1}^n-2P_i^n+P_{i-1}^n\right)\\&=\sum_{k=0}^{n-1}\mathcal{H}_h d_{i,k}^{q,\alpha}\,\mathrm{e}^{-\rho U_i(n-k)\tau}P_i^0-\sum_{k=1}^{n-1}\mathcal{H}_h d_{i,k}^{q,\alpha}P_i^{n-k}+\tau^{\alpha}\mathcal{H}_h f_i^0,\\&\quad 1\leq i\leq M-1,\quad 1\leq n\leq N,\quad q=1,2,3,4. \quad (25)\end{aligned}$$

It is necessary to point out that when $n=1$, the second term on the right-hand side of Eq. (25) vanishes automatically.

3. Stability and convergence analysis

In this section, we do the detailed theoretical analysis for the first order discretization in temporal direction of schemes (22)–(24). Letting $U(x)=\omega$ be a nonnegative constant, we introduce the properties of $l_k^{1,\alpha}$ $(k\geq 0)$ first, and then prove the schemes are unconditionally stable and convergent in the maximum norm.

Lemma 4[31] The coefficients $l_k^{1,\alpha}$ defined by Eq. (18) satisfy

$$l_0^{1,\alpha}=1;\ \ l_k^{1,\alpha}<0,(k\geq 1);\ \ \sum_{k=0}^{n-1}l_k^{1,\alpha}>0;\ \ \sum_{k=0}^{\infty}l_k^{1,\alpha}=0; \quad (26)$$

and

$$\frac{1}{n^{\alpha}\Gamma(1-\alpha)}<\sum_{k=0}^{n-1}l_k^{1,\alpha}=-\sum_{k=n}^{\infty}l_k^{1,\alpha}\leq\frac{1}{n^{\alpha}},\quad n\geq 1. \quad (27)$$

Theorem 1 The finite difference schemes (22)–(24) are unconditionally stable with the assumption $\Re(\rho)\omega\geq 0$.

Proof Assume $\widetilde{P}_i^n$ is the approximate solution of P_i^n which is the exact solution of schemes (22)–(24), and $\widetilde{\varphi}(x_i)$ is the approximation to $\varphi(x_i)$. Let $\varepsilon_i^n=\widetilde{P}_i^n-P_i^n$, $0\leq i\leq M$, $0\leq n\leq N$. From Eqs. (22)–(24), we have the perturbation error equations

$$\begin{aligned}&\mathcal{H}_h\left(d_{i,0}^{1,\alpha}\varepsilon_i^n+\sum_{k=1}^{n-1}d_{i,k}^{1,\alpha}\varepsilon_i^{n-k}-\sum_{k=0}^{n-1}d_{i,k}^{1,\alpha}\,\mathrm{e}^{-\rho\omega(n-k)\tau}\varepsilon_i^0\right)\\&= K_{\alpha}\tau^{\alpha}\delta_x^2\varepsilon_i^n, \quad (28)\\&\quad 1\leq i\leq M-1,\quad 1\leq n\leq N,\\&\quad \varepsilon_i^0=\widetilde{\varphi}(x_i)-\varphi(x_i),\quad 1\leq i\leq M-1, \quad (29)\\&\quad \varepsilon_0^n=\varepsilon_M^n=0,\quad 0\leq n\leq N. \quad (30)\end{aligned}$$

By use of Eq. (17), equation (28) can also be written as

$$\begin{aligned}&\mathcal{H}_h\left(l_0^{1,\alpha}\varepsilon_i^n+\sum_{k=1}^{n-1}\mathrm{e}^{-\rho\omega k\tau}l_k^{1,\alpha}\varepsilon_i^{n-k}-\sum_{k=0}^{n-1}\mathrm{e}^{-\rho\omega n\tau}l_k^{1,\alpha}\varepsilon_i^0\right)\\&= K_{\alpha}\tau^{\alpha}\delta_x^2\varepsilon_i^n. \quad (31)\end{aligned}$$

Multiplying Eq. (31) by $h(-\delta_x^2\overline{\varepsilon}_i^n)$ and summing up for i from 1 to $M-1$, we obtain

$$h\sum_{i=1}^{M-1}\left(-\delta_x^2\overline{\varepsilon}_i^n\right)\left[\left(1+\frac{h^2}{12}\delta_x^2\right)\left(l_0^{1,\alpha}\varepsilon_i^n+\sum_{k=1}^{n-1}\mathrm{e}^{-\rho\omega k\tau}l_k^{1,\alpha}\varepsilon_i^{n-k}-\sum_{k=0}^{n-1}\mathrm{e}^{-\rho\omega n\tau}l_k^{1,\alpha}\varepsilon_i^0\right)\right]=h\sum_{i=1}^{M-1}\left(-K_\alpha\tau^\alpha\right)|\delta_x^2\varepsilon_i^n|^2.$$

Using the summation formula by parts and noticing Eq. (30), we obtain

$$\begin{aligned}
&l_0^{1,\alpha}h\sum_{i=0}^{M-1}\left|\delta_x\varepsilon_{i+1/2}^n\right|^2-l_0^{1,\alpha}\frac{h^2}{12}h\sum_{i=1}^{M-1}\left|\delta_x^2\varepsilon_i^n\right|^2\\
&=-h\sum_{i=0}^{M-1}\sum_{k=1}^{n-1}l_k^{1,\alpha}\left(\delta_x\overline{\varepsilon}_{i+1/2}^n\right)\left(\delta_x\left(\mathrm{e}^{-\rho\omega k\tau}\varepsilon_{i+1/2}^{n-k}\right)\right)\\
&\quad+\frac{h^2}{12}h\sum_{i=1}^{M-1}\sum_{k=1}^{n-1}l_k^{1,\alpha}\left(\delta_x^2\overline{\varepsilon}_i^n\right)\left(\delta_x^2\left(\mathrm{e}^{-\rho\omega k\tau}\varepsilon_i^{n-k}\right)\right)\\
&\quad+h\sum_{i=0}^{M-1}\sum_{k=0}^{n-1}l_k^{1,\alpha}\left(\delta_x\overline{\varepsilon}_{i+1/2}^n\right)\left(\delta_x\left(\mathrm{e}^{-\rho\omega n\tau}\varepsilon_{i+1/2}^0\right)\right)\\
&\quad-\frac{h^2}{12}h\sum_{i=1}^{M-1}\sum_{k=0}^{n-1}l_k^{1,\alpha}\left(\delta_x^2\overline{\varepsilon}_i^n\right)\left(\delta_x^2\left(\mathrm{e}^{-\rho\omega n\tau}\varepsilon_i^0\right)\right)\\
&\quad-K_\alpha\tau^\alpha\|\delta_x^2\varepsilon^n\|^2.
\end{aligned}$$

Then it can be deduced that the following inequality holds

$$\begin{aligned}
l_0^{1,\alpha}\langle\varepsilon^n,\varepsilon^n\rangle\le&-\sum_{k=1}^{n-1}l_k^{1,\alpha}\left|\langle\mathrm{e}^{-\rho\omega k\tau}\varepsilon^{n-k},\varepsilon^n\rangle\right|\\
&+\sum_{k=0}^{n-1}l_k^{1,\alpha}\left|\langle\mathrm{e}^{-\rho\omega n\tau}\varepsilon^0,\varepsilon^n\rangle\right|.
\end{aligned}\tag{32}$$

Let

$$A_1=-\sum_{k=1}^{n-1}l_k^{1,\alpha}\left|\langle\mathrm{e}^{-\rho\omega k\tau}\varepsilon^{n-k},\varepsilon^n\rangle\right|$$

and

$$A_2=\sum_{k=0}^{n-1}l_k^{1,\alpha}\left|\langle\mathrm{e}^{-\rho\omega n\tau}\varepsilon^0,\varepsilon^n\rangle\right|.$$

From the Cauchy–Schwarz inequality and Lemma 4, we have the estimates

$$\begin{aligned}
A_1\le&\frac{1}{2}\sum_{k=1}^{n-1}(-l_k^{1,\alpha})\\
&\times\left(\langle\varepsilon^n,\varepsilon^n\rangle+\langle\mathrm{e}^{-\rho\omega k\tau}\varepsilon^{n-k},\mathrm{e}^{-\rho\omega k\tau}\varepsilon^{n-k}\rangle\right),
\end{aligned}\tag{33}$$

$$A_2\le\frac{1}{2}\sum_{k=0}^{n-1}l_k^{1,\alpha}\left(\langle\varepsilon^n,\varepsilon^n\rangle+\langle\mathrm{e}^{-\rho\omega n\tau}\varepsilon^0,\mathrm{e}^{-\rho\omega n\tau}\varepsilon^0\rangle\right).\tag{34}$$

Combining inequalities (32), (33), and (34) with the assumption $\Re(\rho)\omega\ge0$, it yields that

$$\begin{aligned}
\frac{1}{2}l_0^{1,\alpha}\langle\varepsilon^n,\varepsilon^n\rangle\le&-\frac{1}{2}\sum_{k=1}^{n-1}l_k^{1,\alpha}\langle\varepsilon^{n-k},\varepsilon^{n-k}\rangle+\frac{1}{2}l_0^{1,\alpha}\langle\varepsilon^0,\varepsilon^0\rangle\\
&+\frac{1}{2}\sum_{k=1}^{n-1}l_k^{1,\alpha}\langle\varepsilon^0,\varepsilon^0\rangle.
\end{aligned}\tag{35}$$

Next, we prove

$$\langle\varepsilon^n,\varepsilon^n\rangle\le\langle\varepsilon^0,\varepsilon^0\rangle\tag{36}$$

by mathematical induction. In the case $n=1$, inequality (36) holds according to inequality (35). Suppose that for $s=1,2,\ldots,n-1$,

$$\langle\varepsilon^s,\varepsilon^s\rangle\le\langle\varepsilon^0,\varepsilon^0\rangle\tag{37}$$

holds. When $s=n$, according to inequalities (35) and (37), we have

$$\begin{aligned}
\frac{1}{2}l_0^{1,\alpha}\langle\varepsilon^n,\varepsilon^n\rangle\le&-\frac{1}{2}\sum_{k=1}^{n-1}l_k^{1,\alpha}\langle\varepsilon^0,\varepsilon^0\rangle+\frac{1}{2}l_0^{1,\alpha}\langle\varepsilon^0,\varepsilon^0\rangle\\
&+\frac{1}{2}\sum_{k=1}^{n-1}l_k^{1,\alpha}\langle\varepsilon^0,\varepsilon^0\rangle,
\end{aligned}$$

which means $\langle\varepsilon^n,\varepsilon^n\rangle\le\langle\varepsilon^0,\varepsilon^0\rangle$.

Combining inequality (36) with Lemma 1 and Lemma 2, we conclude that

$$\begin{aligned}
\|\varepsilon^n\|_\infty^2\le&\frac{L}{4}\|\delta_x\varepsilon^n\|^2\le\frac{L}{4}\cdot\frac{3}{2}\langle\varepsilon^n,\varepsilon^n\rangle\le\frac{3L}{8}\langle\varepsilon^0,\varepsilon^0\rangle\\
\le&\frac{3L}{8}\|\delta_x\varepsilon^0\|^2,
\end{aligned}$$

which completes the proof.

Theorem 2 Let P_i^n be the solution of the finite difference schemes (22)–(24), and $P(x_i,t_n)$ be the solution of the problems (8)–(10) with the assumption $\Re(\rho)\omega\ge0$. Denoting $E_i^n=P(x_i,t_n)-P_i^n$, $0\le i\le M$, $0\le n\le N$, then there exists a positive constant C such that

$$\|E^n\|_\infty\le C\left(\tau+h^4\right),\quad 0\le n\le N.$$

Proof According to Eqs. (20) and (22)–(24), we get the error equations

$$\mathcal{H}_h\left(d_{i,0}^{1,\alpha}E_i^n+\sum_{k=1}^{n-1}d_{i,k}^{1,\alpha}E_i^{n-k}\right)=K_\alpha\tau^\alpha\delta_x^2E_i^n+\tau^\alpha R_i^n,\tag{38}$$

$$1\le i\le M-1,\quad 1\le k\le N,$$

$$E_0^n=0,\quad E_M^n=0,\quad 0\le n\le N,\tag{39}$$

$$E_i^0=0,\quad 1\le i\le M-1\tag{40}$$

with $|R_i^n|\le\widetilde{C}(\tau+h^4)$. Multiplying Eq. (38) by $h(-\delta_x^2\overline{E}_i^n)$ and summing up for i from 1 to $M-1$, we have

$$\begin{aligned}
&h\sum_{i=1}^{M-1}\left(-\delta_x^2\overline{E}_i^n\right)\left[\left(1+\frac{h^2}{12}\delta_x^2\right)\left(d_{i,0}^{1,\alpha}E_i^n+\sum_{k=1}^{n-1}d_{i,k}^{1,\alpha}E_i^{n-k}\right)\right]\\
&=hK_\alpha\tau^\alpha\sum_{i=1}^{M-1}\left(-\delta_x^2\overline{E}_i^n\right)\left(\delta_x^2E_i^n\right)+h\tau^\alpha\sum_{i=1}^{M-1}\left(-\delta_x^2\overline{E}_i^n\right)R_i^n.
\end{aligned}\tag{41}$$

From Eq. (17), equation (41) can also be written as

$$h\sum_{i=1}^{M-1}\left(-\delta_x^2\overline{E}_i^n\right)\left(l_0^{1,\alpha}E_i^n+\sum_{k=1}^{n-1}\mathrm{e}^{-\rho\omega k\tau}l_k^{1,\alpha}E_i^{n-k}\right)$$

$$
\begin{aligned}
&+\frac{h^2}{12}h\sum_{i=1}^{M-1}\left(-\delta_x^2\overline{E}_i^n\right)\\
&\times\left(l_0^{1,\alpha}\delta_x^2E_i^n+\sum_{k=1}^{n-1}l_k^{1,\alpha}\delta_x^2\left(\mathrm{e}^{-\rho\omega k\tau}E_i^{n-k}\right)\right)\\
&=-K_\alpha\tau^\alpha h\sum_{i=1}^{M-1}\left|\delta_x^2E_i^n\right|^2-\tau^\alpha h\sum_{i=1}^{M-1}\left(\delta_x^2\overline{E}_i^n\right)R_i^n. \qquad (42)
\end{aligned}
$$

Using the summation formula by parts, we obtain from Eq. (42)

$$
\begin{aligned}
&l_0^{1,\alpha}h\sum_{i=0}^{M-1}\left|\delta_xE_{i+1/2}^n\right|^2\\
&+h\sum_{k=1}^{n-1}l_k^{1,\alpha}\sum_{i=0}^{M-1}\left(\delta_x\overline{E}_{i+1/2}^n\right)\left(\delta_x\,\mathrm{e}^{-\rho\omega k\tau}E_{i+1/2}^{n-k}\right)\\
&-l_0^{1,\alpha}\frac{h^2}{12}h\sum_{i=1}^{M-1}\left|\delta_x^2E_i^n\right|^2\\
&-\frac{h^2}{12}h\sum_{k=1}^{n-1}l_k^{1,\alpha}\sum_{i=1}^{M-1}\left(\delta_x^2\overline{E}_i^n\right)\left(\delta_x^2\,\mathrm{e}^{-\rho\omega k\tau}E_i^{n-k}\right)\\
&=-K_\alpha\tau^\alpha h\sum_{i=1}^{M-1}\left|\delta_x^2E_i^n\right|^2-\tau^\alpha h\sum_{i=1}^{M-1}\left(\delta_x^2\overline{E}_i^n\right)R_i^n,
\end{aligned}
$$

which implies

$$
\begin{aligned}
&l_0^{1,\alpha}\langle E^n,E^n\rangle+\sum_{k=1}^{n-1}l_k^{1,\alpha}\langle\mathrm{e}^{-\rho\omega k\tau}E^{n-k},E^n\rangle\\
&=-K_\alpha\tau^\alpha\|\delta_x^2E^n\|^2-\tau^\alpha h\sum_{i=1}^{M-1}\left(\delta_x^2\overline{E}_i^n\right)R_i^n.
\end{aligned}
$$

Then it can be deduced that

$$
\begin{aligned}
&l_0^{1,\alpha}\langle E^n,E^n\rangle\\
&=\left|-\sum_{k=1}^{n-1}l_k^{1,\alpha}\langle\mathrm{e}^{-\rho\omega k\tau}E^{n-k},E^n\rangle-\tau^\alpha h\sum_{i=1}^{M-1}\left(\delta_x^2\overline{E}_i^n\right)R_i^n\right|\\
&\quad-K_\alpha\tau^\alpha\|\delta_x^2E^n\|^2\\
&\le\left|-\sum_{k=1}^{n-1}l_k^{1,\alpha}\langle\mathrm{e}^{-\rho\omega k\tau}E^{n-k},E^n\rangle\right|+\tau^\alpha h\left|\sum_{i=1}^{M-1}\left(\delta_x^2\overline{E}_i^n\right)R_i^n\right|\\
&\quad-K_\alpha\tau^\alpha\|\delta_x^2E^n\|^2\\
&\le\sum_{k=1}^{n-1}(-l_k^{1,\alpha})\left|\langle\mathrm{e}^{-\rho\omega k\tau}E^{n-k},E^n\rangle\right|+\tau^\alpha h\left|\sum_{i=1}^{M-1}\left(\delta_x^2\overline{E}_i^n\right)R_i^n\right|\\
&\quad-K_\alpha\tau^\alpha\|\delta_x^2E^n\|^2\\
&\le-\frac{1}{2}\sum_{k=1}^{n-1}l_k^{1,\alpha}\left(\langle E^n,E^n\rangle+\langle\mathrm{e}^{-\rho\omega k\tau}E^{n-k},\mathrm{e}^{-\rho\omega k\tau}E^{n-k}\rangle\right)\\
&\quad-K_\alpha\tau^\alpha\|\delta_x^2E^n\|^2+\tau^\alpha h\left|\sum_{i=1}^{M-1}\left(\delta_x^2\overline{E}_i^n\right)R_i^n\right| \qquad (43)
\end{aligned}
$$

with the Cauchy-Schwarz inequality being used.

Let

$$
B=\tau^\alpha h\left|\sum_{i=1}^{M-1}\left(\delta_x^2\overline{E}_i^n\right)R_i^n\right|.
$$

It is observed that

$$
\begin{aligned}
B&\le\tau^\alpha h\sum_{i=1}^{M-1}\left|\left(\delta_x^2\overline{E}_i^n\right)R_i^n\right|\\
&\le\tau^\alpha hK_\alpha\sum_{i=1}^{M-1}\left|\delta_x^2\overline{E}_i^n\right|^2+\tau^\alpha h\frac{1}{4K_\alpha}\sum_{i=1}^{M-1}|R_i^n|^2\\
&=K_\alpha\tau^\alpha\|\delta_x^2E^n\|^2+\frac{\tau^\alpha}{4K_\alpha}\|R^n\|^2. \qquad (44)
\end{aligned}
$$

Since $|R_i^n|\le\widetilde{C}\left(\tau+h^4\right)$, it can be obtained that

$$
\|R^n\|^2\le L\widetilde{C}^2(\tau+h^4)^2. \qquad (45)
$$

Substituting expression (44) into expression (43), and noticing inequality (45) with the assumption $\Re(\rho)\omega\ge0$, we have

$$
\begin{aligned}
l_0^{1,\alpha}\langle E^n,E^n\rangle&\le-\frac{1}{2}\sum_{k=1}^{n-1}l_k^{1,\alpha}\langle E^n,E^n\rangle-\frac{1}{2}\sum_{k=1}^{n-1}l_k^{1,\alpha}\langle E^{n-k},E^{n-k}\rangle\\
&\quad+\frac{C_1\tau^\alpha}{2}(\tau+h^4)^2, \qquad (46)
\end{aligned}
$$

where $C_1=\widetilde{C}^2L/2K_\alpha$. According to Lemma 4, there exists

$$
0<-\frac{1}{2}\sum_{k=1}^{n-1}l_k^{1,\alpha}<\frac{1}{2},
$$

and then it is derived from inequality (46) that

$$
\langle E^n,E^n\rangle\le-\sum_{k=1}^{n-1}l_k^{1,\alpha}\langle E^{n-k},E^{n-k}\rangle+C_1\tau^\alpha(\tau+h^4)^2. \qquad (47)
$$

In the following, we prove

$$
\langle E^n,E^n\rangle\le\left(\sum_{k=0}^{n-1}l_k^{1,\alpha}\right)^{-1}C_1\tau^\alpha(\tau+h^4)^2 \qquad (48)
$$

by mathematical induction.

For $n=1$, inequality (48) holds by inequality (47). Suppose

$$
\begin{aligned}
&\langle E^s,E^s\rangle\le\left(\sum_{k=0}^{s-1}l_k^{1,\alpha}\right)^{-1}C_1\tau^\alpha(\tau+h^4)^2,\\
&s=1,2,\ldots,n-1. \qquad (49)
\end{aligned}
$$

Then for $s=n$, by using inequalities (47) and (49) we conclude that

$$
\begin{aligned}
&\langle E^n,E^n\rangle\\
&\le-\sum_{k=1}^{n-1}l_k^{1,\alpha}\left(\sum_{m=0}^{n-k-1}l_m^{1,\alpha}\right)^{-1}C_1\tau^\alpha\left(\tau+h^4\right)^2+C_1\tau^\alpha\left(\tau+h^4\right)^2\\
&\le-\left(\sum_{k=0}^{n-1}l_k^{1,\alpha}\right)^{-1}\sum_{k=1}^{n-1}l_k^{1,\alpha}C_1\tau^\alpha\left(\tau+h^4\right)^2+C_1\tau^\alpha(\tau+h^4)^2\\
&=\left(1-\frac{\sum_{k=1}^{n-1}l_k^{1,\alpha}}{\sum_{k=0}^{n-1}l_k^{1,\alpha}}\right)C_1\tau^\alpha(\tau+h^4)^2\\
&=\left(\sum_{k=0}^{n-1}l_k^{1,\alpha}\right)^{-1}C_1\tau^\alpha(\tau+h^4)^2. \qquad (50)
\end{aligned}
$$

Finally, according to inequalities (50), (27), Lemma 1 and Lemma 2, we derive

$$\begin{aligned}\|E^n\|_\infty^2 &\le \frac{L}{4}\|\delta_x E^n\|^2\\ &\le \frac{3L}{8}\langle E^n, E^n\rangle\\ &\le \frac{3L}{8}\left(\sum_{k=0}^{n-1} l_k^{1,\alpha}\right)^{-1} C_1\tau^\alpha(\tau+h^4)^2\\ &\le \frac{3L}{8}n^\alpha\Gamma(1-\alpha)C_1\tau^\alpha(\tau+h^4)^2\\ &\le [C(\tau+h^4)]^2,\end{aligned}$$

where $C=\sqrt{(3L/8)T^\alpha\Gamma(1-\alpha)C_1}$. This completes the proof.

4. Numerical examples

In this section, firstly we test some numerical examples to demonstrate the effectiveness of the schemes (22)–(24), and verify the theoretical results including convergence orders and numerical stability. The numerical errors is computed in the maximum norm, *i.e.*,

$$\|E^N\|_\infty := \max_{1\le i\le M-1}|P(x_i,t_N)-P_i^N|.$$

Then the backward fractional Feynman–Kac equation with Dirac delta function as the initial condition is simulated. By making use of the algorithm of numerical inversion of Laplace transforms,[36] we obtain the joint PDF $P(x,A,t)$, and then the marginal PDFs of A and x, respectively. In particular, the case $U(x)=0$ is considered, when equation (8) reduces to the fractional Fokker–Planck equation.[37–40] Comparing its solution with the marginal PDF of x, it is further confirmed the reliability of our numerical methods.

4.1. Numerical results for $P(x,t)$ with ρ being a constant

In the following two examples, we choose $U(x)=1$ and x, respectively.

Example 1 Consider

$$\begin{aligned}&{}^sD_t^\alpha\left[P(x,t)-\mathrm{e}^{-(1+i)t}P(x,0)\right]\\ &=0.5\frac{\partial^2}{\partial x^2}P(x,t)+\frac{\Gamma(4+\alpha)}{\Gamma(4)}\mathrm{e}^{-(1+i)t}t^3\sin(\pi x)\\ &\quad+0.5\pi^2\left(t^{3+\alpha}+1\right)\mathrm{e}^{-(1+i)t}\sin(\pi x),\quad 0<t\le 1,\ 0<x<1,\\ &\quad P(x,0)=\sin(\pi x),\quad 0<x<1,\\ &\quad P(0,t)=0,\ P(1,t)=0,\quad 0\le t\le 1,\end{aligned}$$

whose exact solution is known and is given by

$$P(x,t)=\mathrm{e}^{-(1+i)t}\left(t^{3+\alpha}+1\right)\sin(\pi x).$$

In Table 1, an optimal step size ratio in temporal and spatial directions is adopted for Example 1 with $q=1$. As h and τ vary, the errors and convergence orders are reported in the table, which implies that the convergence orders in temporal and spatial directions are about one and four, respectively. It is in good agreement with the theoretical analysis.

Table 2 displays the computational results with an optimal step size ratio in temporal and spatial directions for Example 1 with $q=2$. It can be concluded from this table that the convergence orders with respect to time and space are approximately two and four, respectively. It agrees well with the theoretical results.

Table 1. The maximum errors and convergence orders with $q=1$ and an optimal step size ratio $\tau=h^4$ (Example 1).

h	$\alpha=0.2$	Order	$\alpha=0.5$	Order	$\alpha=0.8$	Order
1/2	0.0184	–	0.0217	–	0.0279	–
1/4	0.0011	4.0641	0.0013	4.0611	0.0017	4.0367
1/8	6.5910×10^{-5}	4.0609	7.8904×10^{-5}	4.0423	1.0316×10^{-4}	4.0426
1/10	2.6942×10^{-5}	4.0091	3.2266×10^{-5}	4.0074	4.2201×10^{-5}	4.0057

Table 2. The maximum errors and convergence orders with $q=2$ and an optimal step size ratio $\tau=h^2$ (Example 1).

h	$\alpha=0.2$	Order	$\alpha=0.5$	Order	$\alpha=0.8$	Order
1/10	2.7752×10^{-5}	–	3.5587×10^{-5}	–	5.1361×10^{-5}	–
1/20	1.7312×10^{-6}	4.0027	2.2245×10^{-6}	3.9998	3.2177×10^{-6}	3.9966
1/40	1.0815×10^{-7}	4.0007	1.3903×10^{-7}	4.0000	2.0122×10^{-7}	3.9992
1/80	6.7586×10^{-9}	4.0002	8.6896×10^{-9}	4.0000	1.2578×10^{-8}	3.9998

Example 2 We now consider

$$\begin{aligned}&{}^sD_t^\alpha\left[P(x,t)-\mathrm{e}^{-(1+i)xt}P(x,0)\right]\\ &=0.5\frac{\partial^2}{\partial x^2}P(x,t)+\frac{\Gamma(4+\alpha)}{\Gamma(4)}\mathrm{e}^{-(1+i)xt}t^3\sin(\pi x)\\ &\quad-0.5\mathrm{e}^{-(1+i)xt}\left(t^{3+\alpha}+1\right)\left((1+i)^2t^2\sin(\pi x)\right.\\ &\quad\left.-2\pi(1+i)t\cos(\pi x)-\pi^2\sin(\pi x)\right),\\ &\quad 0<t\le 1,\ 0<x<1,\\ &\quad P(x,0)=\sin(\pi x),\quad 0<x<1,\\ &\quad P(0,t)=0,\ P(1,t)=0,\quad 0\le t\le 1,\end{aligned}$$

whose exact solution is known and is given by

$$P(x,t)=\mathrm{e}^{-(1+i)xt}\left(t^{3+\alpha}+1\right)\sin(\pi x).$$

Table 3 shows the numerical errors and convergence or-

ders in temporal direction for Example 2 with $q = 3$. Let the step size h be fixed and small enough such that the dominating error arises from the approximation of the time derivative. Varying the step size in time, the numerical results are listed in this table, which is in accord with the theoretical analysis.

Tables 4–6 record the comparisons of schemes (22)–(24) with the scheme (2.12) in Ref. [31] for Example 2 with $q = 4$. Taking an optimal step size ratio in temporal and spatial directions, these results report the convergence orders of schemes (22)–(24) with respect to time and space are both about four, which confirms the theoretical results. It also can be seen that even on the more coarse mesh schemes (22)–(24) get the smaller errors. These numerical results show that our method is not only reliable but also more efficient.

Table 3. The maximum errors and convergence orders in temporal direction with $q = 3$ and $h = 1/1000$ (Example 2).

τ	$\alpha = 0.2$	Order	$\alpha = 0.5$	Order	$\alpha = 0.8$	Order
1/10	4.0581×10^{-5}	–	1.5822×10^{-4}	–	4.1108×10^{-4}	–
1/20	5.0826×10^{-6}	2.9972	1.9862×10^{-5}	2.9938	5.1656×10^{-5}	2.9924
1/40	6.3591×10^{-7}	2.9987	2.4876×10^{-6}	2.9972	6.4710×10^{-6}	2.9969
1/80	7.9535×10^{-8}	2.9992	3.1123×10^{-7}	2.9987	8.0969×10^{-7}	2.9985
1/160	9.9561×10^{-9}	2.9979	3.8898×10^{-8}	3.0002	1.0126×10^{-7}	2.9993

Table 4. Comparisons of errors and convergence orders obtained by schemes (22)–(24) and scheme (2.12) in Ref. [31] with $\alpha = 0.1$, $q = 4$ and an optimal step size ratio for τ and h (Example 2).

Schemes (22)–(24)				Scheme (2.12) in Ref. [31]			
τ	h	$\|E^N\|_\infty$	Order	τ	h	$\|E^N\|_\infty$	Order
1/10	1/10	1.0794×10^{-4}	–	1/10	1/100	1.1563×10^{-4}	–
1/20	1/20	6.7472×10^{-6}	3.9998	1/20	1/400	7.2278×10^{-6}	3.9998
1/40	1/40	4.2127×10^{-7}	4.0015	1/40	1/1600	4.5173×10^{-7}	4.0000
1/80	1/80	2.6336×10^{-8}	3.9996	1/80	1/6400	2.7781×10^{-8}	4.0233

Table 5. Comparisons of errors and convergence orders obtained by schemes (22)–(24) and scheme (2.12) in Ref. [31] with $\alpha = 0.5$, $q = 4$ and an optimal step size ratio for τ and h (Example 2).

Schemes (22)–(24)				Scheme (2.12) in Ref. [31]			
τ	h	$\|E^N\|_\infty$	Order	τ	h	$\|E^N\|_\infty$	Order
1/10	1/10	9.7935×10^{-5}	–	1/10	1/100	1.0990×10^{-4}	–
1/20	1/20	6.0897×10^{-6}	4.0074	1/20	1/400	6.8693×10^{-6}	3.9998
1/40	1/40	3.8077×10^{-7}	3.9994	1/40	1/1600	4.2926×10^{-7}	4.0003
1/80	1/80	2.3789×10^{-8}	4.0006	1/80	1/6400	2.6565×10^{-8}	4.0143

Table 6. Comparisons of errors and convergence orders obtained by schemes (22)–(24) and scheme (2.12) in Ref. [31] with $\alpha = 0.9$, $q = 4$ and an optimal step size ratio for τ and h (Example 2).

Schemes (22)–(24)				Scheme (2.12) in Ref. [31]			
τ	h	$\|E^N\|_\infty$	Order	τ	h	$\|E^N\|_\infty$	Order
1/10	1/10	8.6476×10^{-5}	–	1/10	1/100	1.0487×10^{-4}	–
1/20	1/20	5.3294×10^{-6}	4.0203	1/20	1/400	6.4844×10^{-6}	4.0154
1/40	1/40	3.3188×10^{-7}	4.0052	1/40	1/1600	4.0409×10^{-7}	4.0042
1/80	1/80	2.0716×10^{-8}	4.0018	1/80	1/6400	2.5510×10^{-8}	3.9855

Graphs of the modulus of errors for Example 2 with $q = 4$ and $\alpha = 0.4$ are plotted in Fig. 1. From these figures, we can find intuitively that, as the step sizes h and τ are reduced, the maximum of the modulus of the errors decreases gradually and approaches zero, which manifests the convergence of the presented algorithms.

4.2. Simulations with Dirac delta function as the initial condition

In this subsection, the backward fractional Feynman–Kac equation (8) with a zero forcing function and Dirac delta function as the initial condition is simulated. The Dirac delta function is defined by the limit of the sequence of Gaussians

$$\delta_a(x) = \frac{1}{2\sqrt{a\pi}} \exp\left(-\frac{x^2}{4a}\right) \quad \text{as} \quad a \to 0. \tag{51}$$

For numerically getting the joint PDF $P(x,A,t)$, the notation $P(x,\rho,t)$ is reused instead of $P(x,t)$.

Example 3 Consider

$$ {}^{s}D_t^{\alpha}\left[P(x,\rho,t) - \mathrm{e}^{-\rho U(x)t}P(x,\rho,0)\right] = 0.5\frac{\partial^2}{\partial x^2}P(x,\rho,t) \quad 0 < t \le T,\ 0 < x < 1,$$

$$P(x,\rho,0)=\delta_a(x-0.5),\quad 0<x<1,$$
$$P(0,\rho,t)=0, P(1,\rho,t)=0,\quad 0\le t\le T,$$

where $U(x)$ is taken as

$$U(x)=\begin{cases}1, & x\in(0.5,1),\\ 0, & \text{otherwise};\end{cases} \tag{52}$$

or

$$U(x)=\begin{cases}1, & x\in(0.25,0.75),\\ 0, & \text{otherwise};\end{cases} \tag{53}$$

or

$$U(x)=1,\quad x\in(0,1). \tag{54}$$

Suppose the joint PDF $P(x,A,t)$ is a real function of A with $P(x,A,t)=0$ for $A<0$. The Laplace transform and its inversion formula are defined as

$$P(x,\rho,t)=\mathscr{L}\{P(x,A,t)\}=\int_0^{\infty}P(x,A,t)\,\mathrm{e}^{-\rho A}\,\mathrm{d}A,$$
$$\rho=\nu+\mathrm{i}w;$$
$$P(x,A,t)=\mathscr{L}^{-1}\{P(x,\rho,t)\}$$
$$=\frac{1}{2\pi\mathrm{i}}\int_{\nu-i\infty}^{\nu+i\infty}P(x,A,t)\,\mathrm{e}^{\rho A}\,\mathrm{d}\rho,$$

where $\nu>0$ is arbitrary, but is greater than the real parts of all the singularities of $P(x,\rho,t)$.

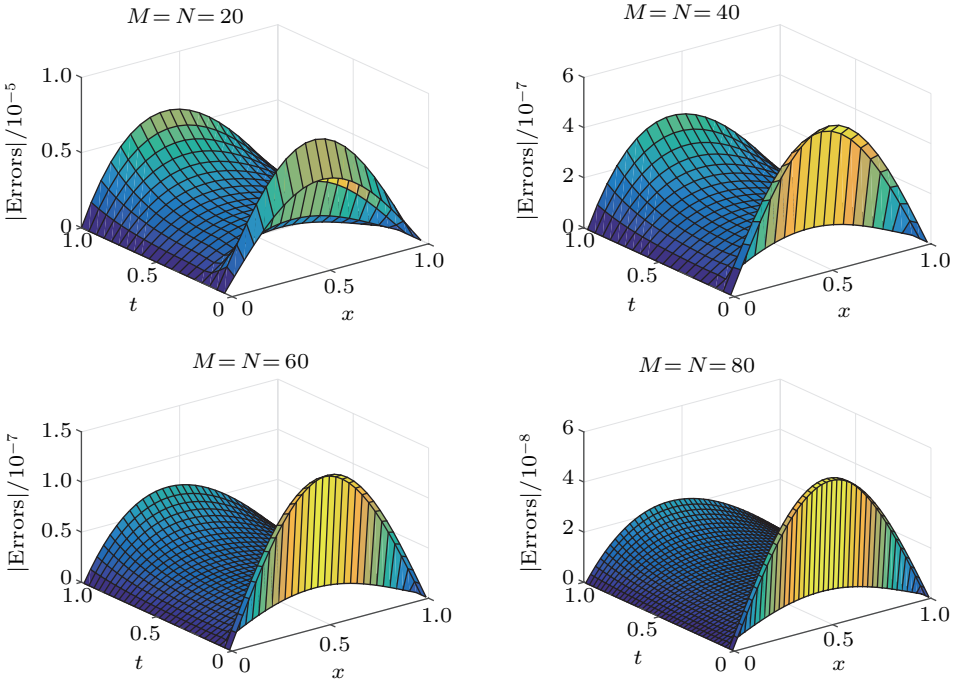


Fig. 1. Evolution of the modulus of errors with $q=4$, $\alpha=0.4$, and four different step sizes (Example 2).

We take $a=0.0005$ in Eq. (51) to get the approximation of Dirac delta function in numerical computations. Using the algorithm of numerical inversion of Laplace transforms,[36] we numerically get the joint PDF $P(x,A,t)$ by taking

$$\rho_k=\nu+\mathrm{i}\frac{\pi}{A}k \text{ with } \nu=\frac{18.4}{2A},\ \mathrm{i}=\sqrt{-1},\ k=0,1,2,\ldots,35.$$

Then the two marginal PDFs

$$J(A)=\int_{-\infty}^{+\infty}P(x,A,t)\,\mathrm{d}x$$

and

$$K(x)=\int_{-\infty}^{+\infty}P(x,A,t)\,\mathrm{d}A$$

are derived by the composite trapezoidal formula.

For generating Figs. 2–5, the procedure can be executed as follows.

Step 1 For each fixed α, A, and ρ_k $(k=0,1,\ldots,35)$, by employing schemes (22)–(24) with $q=4$, $\tau=h=1/200$, we get $P(x,\rho_k,t)$ at time T.

Step 2 According to the numerical method,[36] we obtain $P(x,A,t)$.

Step 3 By making use of the composite trapezoidal formula, we get the marginal PDF $J(A)$.

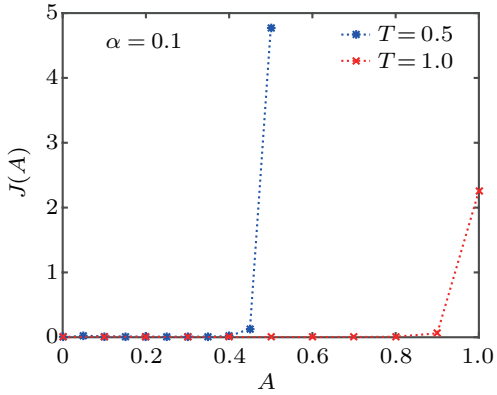


Fig. 2. $J(A)$ for Eq. (22) with $U(x)$ defined in Eq. (52).

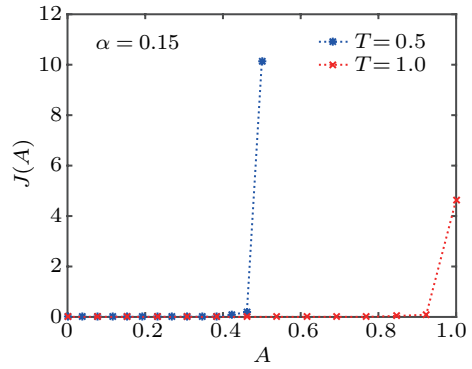


Fig. 3. $J(A)$ for Eq. (22) with $U(x)$ defined in Eq. (53).

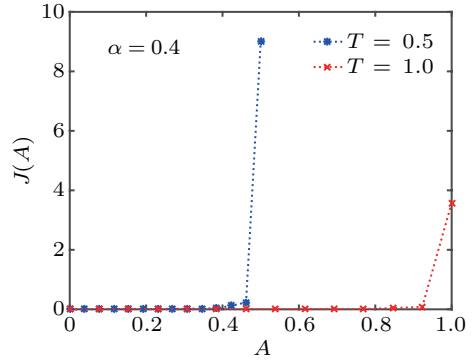


Fig. 4. $J(A)$ for Eq. (22) with $U(x)$ defined in Eq. (53).

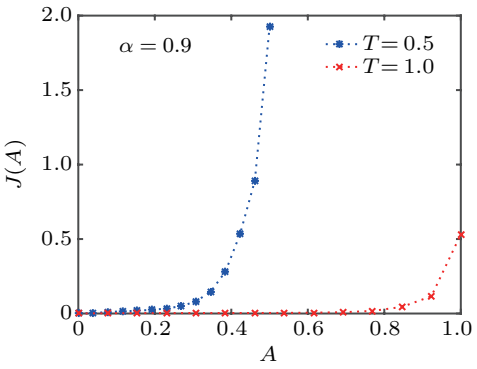


Fig. 5. $J(A)$ for Eq. (22) with $U(x)$ defined in Eq. (53).

Figures 2–5 present the curves of the marginal PDF $J(A)$, where we can see the areas under the curves at time $T = 0.5$ and $T = 1.0$ are almost the same. It implies the conservation of probability.

The procedure of generating Figs. 6–8 can be executed as follows.

Step 1 Take $U(x)$ as defined in Eq. (54). For each fixed α, A, and ρ_k $(k = 0,1,\ldots,35)$, by employing schemes (22)–(24) with $q = 4$, $\tau = h = 1/200$, we get $P(x,\rho_k,t)$ at time $T = 0.2$.

Step 2 According to the numerical method,[36] we obtain $P(x,A,t)$.

Step 3 By making use of the composite trapezoidal formula, we have the marginal PDF $K(x)$.

Step 4 Letting $U(x) = 0$ and using schemes (22)–(24) with $q = 4$, we obtain the solution of the fractional Fokker–Planck equation $KK(x)$.

Figures 6–8 depict the marginal PDF $K(x)$, as well as the numerical solution of fractional Fokker–Planck equation $KK(x)$. We can see $K(x)$ coincides with $KK(x)$, which further verified the effectiveness of the proposed schemes.

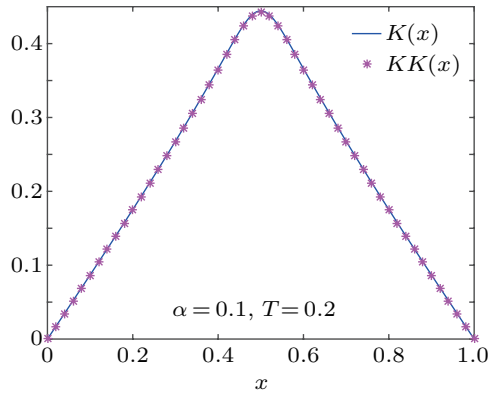


Fig. 6. $K(x)$ and $KK(x)$ for Eq. (22), respectively.

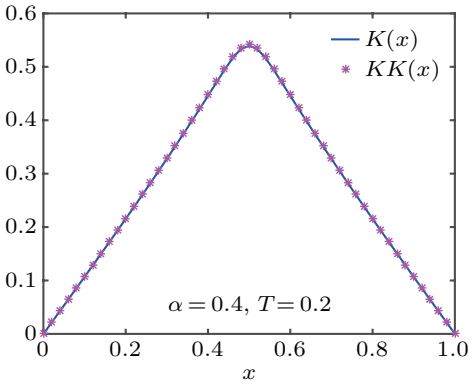


Fig. 7. $K(x)$ and $KK(x)$ for Eq. (22), respectively.

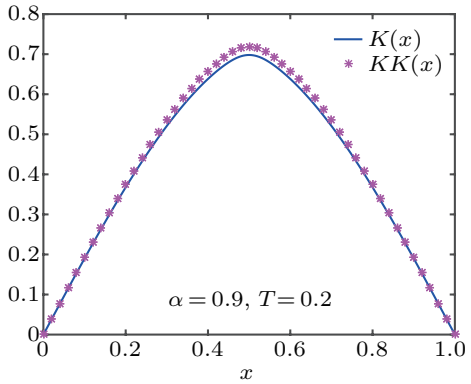


Fig. 8. $K(x)$ and $KK(x)$ for Eq. (22), respectively.

5. Conclusion

In this paper, compact finite difference schemes for solving the backward fractional Feynman–Kac equation are proposed. These schemes are of the q-th $(q = 1,2,3,4)$ order accuracy in time and the fourth order accuracy in space, respectively.

By generalizing the inner product in Ref. [18] to complex space, we prove that the first-order time discretization

scheme is unconditionally stable and convergent in maximum norm. For all the schemes proposed, from first to fourth order approximations in temporal direction, abundant numerical experiments are carried out to verify the theoretical analysis and their effectiveness. Moreover, the derived errors and convergence orders are compared with the corresponding results obtained in Ref. [31], which shows that the method in this work is more accurate and efficient. Also, the problem with Dirac delta function as the initial condition is simulated. By employing the algorithm of numerical inversion of Laplace transforms[36] and the composite trapezoidal formula, we draw the curves of the marginal PDFs, as well as the numerical solution of the fractional Fokker–Planck equation, which further confirm the effectiveness of our methods.

References

[1] Comtet A, Desbois J and Texier C 2005 *J. Phys. A: Math. Gen.* **38** R341
[2] Foltin G, Oerding K, Rácz Z, Workman R and Zia R 1994 *Phys. Rev. E* **50** R639
[3] Hummer G and Szabo A 2001 *Proc. Natl. Acad. Sci. USA* **98** 3658
[4] Baule A and Friedrich R 2006 *Phys. Lett. A* **350** 167
[5] Majumdar S and Bray A 2002 *Phys. Rev. E* **65** 051112
[6] Yor M 2001 *Exponential Functionals of Brownian Motion and Related Processes* (Springer Science & Business Media) pp. 182–203
[7] Kac M 1949 *Trans. Am. Math. Soc.* **65** 1
[8] Rueangkham N and Modchang C 2016 *Chin. Phys. B* **25** 048201
[9] Hu W and Shao Y 2014 *Acta Phys. Sin.* **63** 238202 (in Chinese)
[10] Abdelwahed H, El-Shewy E and Mahmoud A 2017 *Chin. Phys. Lett.* **34** 035202
[11] Agmon N 1984 *J. Chem. Phys.* **81** 3644
[12] Carmi S, Turgeman L and Barkai E 2010 *J. Stat. Phys.* **141** 1071
[13] Carmi S and Barkai E 2011 *Phys. Rev. E* **84** 061104
[14] Turgeman L, Carmi S and Barkai E 2009 *Phys. Rev. Lett.* **103** 190201
[15] Friedrich R, Jenko F, Baule A and Eule S 2006 *Phys. Rev. Lett.* **96** 230601
[16] Chen M, Deng W and Wu Y 2013 *Appl. Numer. Math.* **70** 22
[17] Chen S, Liu F, Zhuang P and Anh V 2009 *Appl. Math. Model.* **33** 256
[18] Gao G and Sun Z 2011 *J. Comput. Phys.* **230** 586
[19] Meerschaert M and Tadjeran C 2006 *Appl. Numer. Math.* **56** 80
[20] Sun Z and Wu X 2006 *Appl. Numer. Math.* **56** 193
[21] Deng W 2008 *SIAM J. Numer. Anal.* **47** 204
[22] Ervin V and Roop J 2006 *Numer. Methods Partial Differential Equations* **22** 558
[23] Jiang Y and Ma J 2011 *J. Comput. Appl. Math.* **235** 3285
[24] Liu Y, Li H, Gao W, He S and Fang Z 2014 *Sci. World J.* **2014** 141467
[25] Liu Y, Fang Z, Li H and He S 2014 *Appl. Math. Comput.* **243** 703
[26] Liu F, Zhuang P, Turner I, Burrage K and Anh V 2014 *Appl. Math. Model.* **38** 3871
[27] Feng L, Zhuang P, Liu F and Turner I 2015 *Appl. Math. Comput.* **257** 52
[28] Zhao J, Li H, Fang Z and Liu Y 2019 *Mathematics* **7** 600
[29] Li C, Zeng F and Liu F 2012 *Fract. Calc. Appl. Anal.* **15** 383
[30] Li X and Xu C 2009 *SIAM J. Numer. Anal.* **47** 2108
[31] Deng W, Chen M and Barkai E 2015 *J. Sci. Comput.* **62** 718
[32] Chen M and Deng W 2013 *ESAIM Math. Model. Numer. Anal.* **49** 373
[33] Sun Z 2009 *The Method of Order Reduction and Its Application to the Numerical Solutions of Partial Differential Equations* (Beijing: Science Press) p. 126
[34] Liao H and Sun Z 2010 *Numer. Methods Partial Differential Equations* **26** 37
[35] Chen M and Deng W 2014 *Commun. Comput. Phys.* **16** 516
[36] Abate J 1995 *ORSA J. Comput.* **7** 36
[37] Barkai E 2001 *Phys. Rev. E* **63** 046118
[38] Barkai E, Metzler R and Klafter J 2000 *Phys. Rev. E* **61** 132
[39] Metzler R and Klafter J 2000 *Phys. Rep.* **339** 1
[40] Metzler R, Barkai E and Klafter J 1999 *Phys. Rev. Lett.* **82** 3653